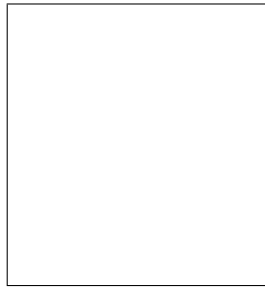


THE FIRST FEW FB⁻¹; POTENTIAL FOR OBSERVATION OF PHYSICS BEYOND THE STANDARD MODEL

R. BELLAN, on behalf of ATLAS and CMS Collaborations
European Organisation for Nuclear Research (CERN), Geneva, Switzerland



An important part of the ATLAS and CMS program is to search for new physics beyond the Standard Model. Some of the main ongoing studies are presented by signature, with particular emphasis on those channels already observable with the first collected data. Here only non-super-symmetric models are presented, as susy models are discussed elsewhere¹.

1 Introduction

LHC will offer the possibility to observe or set limits on new physics beyond the Standard Model (SM), using relatively few data. Many models can suddenly be investigated, although early data may not be enough to identify the model that describes the signal.

In the following sections the signatures of some of the main searches at LHC are discussed.

2 Jet Final States

Inclusive di-jet production ($pp \rightarrow 2 \text{ jets} + \text{anything}$) is the dominant LHC process. To lowest order it arises from the $2 \rightarrow 2$ QCD scattering of partons in which only coloured particles are involved in the initial, intermediate and final states.

Di-jet resonances and contact interactions are the two major signals of new physics with di-jets². Di-jet resonances produce compelling signals of a new particle at a mass M , but require that the incoming parton-parton collision energy to be close to that mass (which must be kinematically accessible). Contact interactions produce more ambiguous signals but come from an energy scale of new physics, Λ , which can be significantly larger than the available collision energy, thus allowing to probe a wider energy spectra. In both cases the observables used to study such processes are very simple. In the inclusive jets analysis the number of jets inside an η window are counted as a function of the jet p_T . For the di-jets study, the two jets

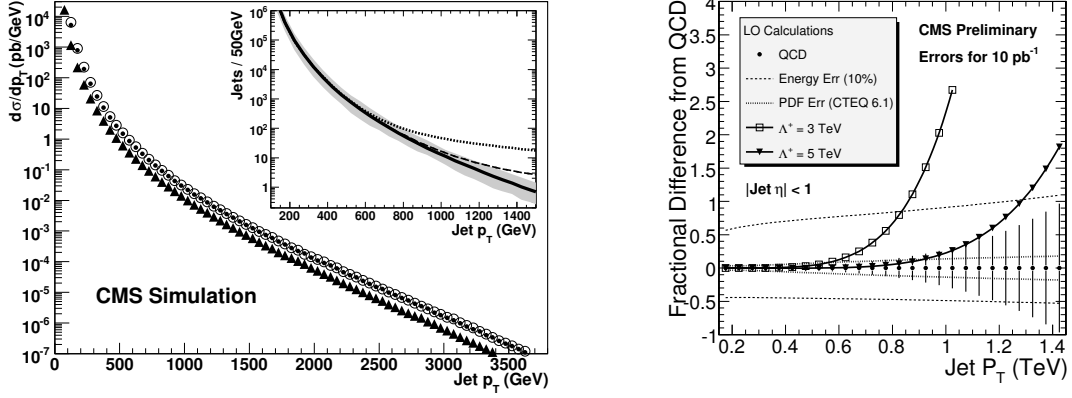


Figure 1: (Left) Inclusive jet differential cross section expected from QCD for $|\eta| < 1$ as a function of jet p_T for generated jets (points), jets (triangles), and corrected jets (open circles). The inset shows the number of generated jets for an integrated luminosity of 10 pb^{-1} . The size of a 10% uncertainty in the jet energy scale (shaded band) is shown centred on the QCD background (solid). The signal from a contact interaction is shown for scale $\Lambda^+ = 3 \text{ TeV}$ (dotted) and $\Lambda^+ = 5 \text{ TeV}$ (dashed). (Right) Fractional difference with respect to QCD as a function of jet momentum. This variable unambiguously shows the discrepancy between the expected QCD background and the signal (Λ^+) for jet- p_T above 1 TeV.

with highest p_T , and inside a given pseudorapidity region, are selected and counted as a function of the invariant mass of the di-jet system.

2.1 Sensitivity to Contact Interactions: Inclusive Jet- p_T Study

New physics at a scale above the energy scale of the process can be effectively modelled as a contact interaction. The canonical contact interaction studied in hadron collisions arises from the following left-left isoscalar colour-singlet term which is added to the QCD Lagrangian³:

$$L_{qq} = \frac{Ag^2}{2\Lambda^2} (\bar{q}_L \gamma^\mu q_L) (\bar{q}_L \gamma_\mu q_L) \quad (1)$$

where $A = \pm 1$ determines the sign of the interference with QCD, Λ is the contact interaction scale and the square of the coupling g^2 is by convention set equal to $4\pi\alpha_s$. Λ^\pm is a compact notation commonly used to include the choice $A = \pm 1$.

Contact interactions produce a rise in rate, relative to QCD, at high inclusive jet p_T as shown in Figure 1. The figure shows the jet rates, expected for an integrated luminosity of 10 pb^{-1} , using a simulation of the CMS experiment. A contact interaction with a scale of $\Lambda^+ = 3 \text{ TeV}$ clearly produces a large rate compared to QCD expectation for jet $p_T > 1 \text{ TeV}$, even taking into account a 10% energy scale uncertainty.

2.2 Sensitivity to di-Jets Resonances: Di-Jet Mass Spectrum Study

Many models predict narrow di-jet resonances⁴. In Figure 2 the cross section for an excited quark di-jet resonance to the statistical uncertainties expected on the QCD di-jet background are compared for a luminosity scenario of 10 pb^{-1} . The normalisation of the excited quark signal come from the lowest order calculation. Figure 2 illustrates that the di-jets channel is sensitive to an excited quark signal up to several TeV. With only 10 pb^{-1} a 2 TeV excited quark signal begins to emerge above the statistical error bars with a total significance of 4.1, neglecting systematic uncertainties.

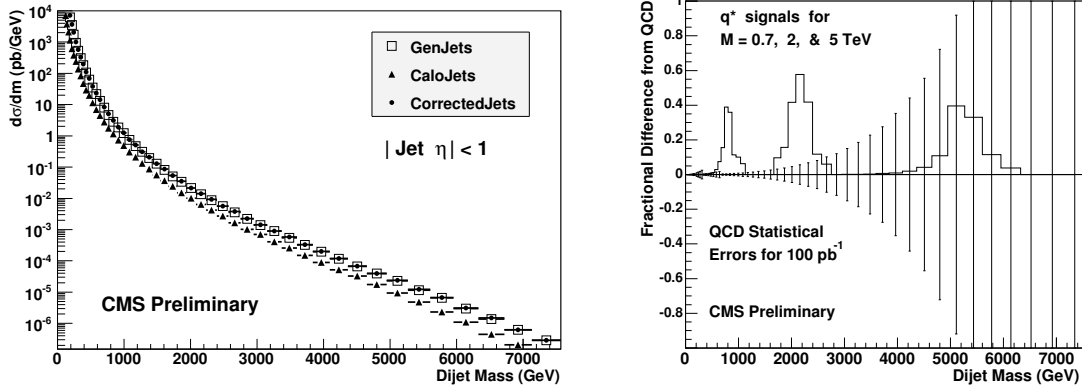


Figure 2: (Left) Di-jets differential cross section expected from QCD for $|\eta| < 1$ as a function of the di-jets invariant mass, for generated jets (points), jets (triangles), and corrected jets (open boxes). (Right) Fractional difference with respect to QCD as a function of di-jets invariant mass, in case of excited quark signal.

3 High Invariant Mass of di-Lepton Final States

In a hadron collider the final states with leptons are a clear signature for many processes, in particular di-lepton final states are naturally the best candidate for discovery of new physics beyond Standard Model. Many models predict either resonances or deviation from the SM differential cross section ($d\sigma/dm_{ll}$) of the process⁴.

The main characteristics of the signal are the high momenta of the leptons, which are also isolated, and the large invariant mass of the lepton pair. The most important background is the Drell-Yan process, although its cross section is vanishing at the energy scale at which new physics is expected. The same signature is shared by many models and this would make difficult the identification of the correct theory using only early data. From the experimental point of view, due to the characteristics of the particles in the final state, the detection, reconstruction and identification of such leptons can be at the limits of the performance of the apparatus, depending on the energy scale at which the new process arises. Therefore a high-level understanding of the alignment⁵ and calibration⁶ of the detector is fundamental for the discovery.

3.1 Resonances in Final States: New Neutral Gauge Bosons

Additional heavy neutral gauge bosons (Z') are predicted in many superstring-inspired^{7,8} and grand unified theories⁹, as well as in dynamical symmetry breaking¹⁰ and little Higgs¹¹ models. However, there are no reliable theoretical predictions of the Z' mass scale. Current lower limits on the Z' mass are (depending on the model) of the order of 600 – 900 GeV/ c^2 ¹².

The Z' most frequently discussed and whose properties are representative of a broad class of extra gauge bosons are:

- Z_{SSM} within the Sequential Standard Model (SSM), which has the same couplings as the Standard Model Z^0 .
- Z_ψ , Z_η and Z_χ , arising in E_6 and $SO(10)$ GUT groups.
- Z_{LRM} and Z_{ALRM} , arising in the framework of the so-called left-right and alternative left-right models.

The LHC offers the opportunity to search for Z' bosons in a mass range significantly larger than 1 TeV/ c^2 , already with the first data⁵. In Figure 3 the summary plot shows that already with 100 pb⁻¹ a region not yet explored by Tevatron experiments can be studied.

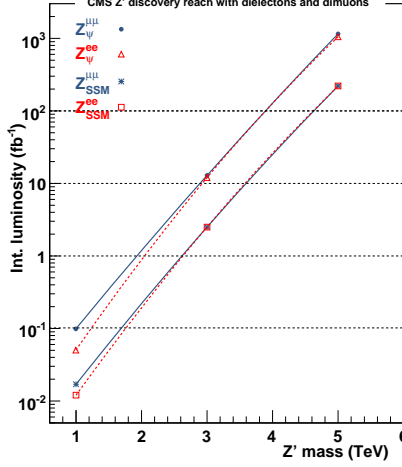


Figure 3: Z' discovery reach for two of the models studied in the di-lepton channels at CMS experiment. The reach of the rest of the models studied is within the band defined by Z_{SSM} and Z_ψ .

The Z' is not the only neutral vector boson that can be seen in leptonic channels. Randall-Sundrum (RS) models¹³ predicts massive Kaluza-Klein (KK) modes of the graviton (G_{RS}).

Most collider physics phenomenology done with warped extra dimensions so far is based upon one very specific model, the original simple scenario called RS1. In RS1, the Standard Model is replaced at TeV scale by a new effective theory in which gravity is still very weak, but there are exotic heavy spin-2 particles.

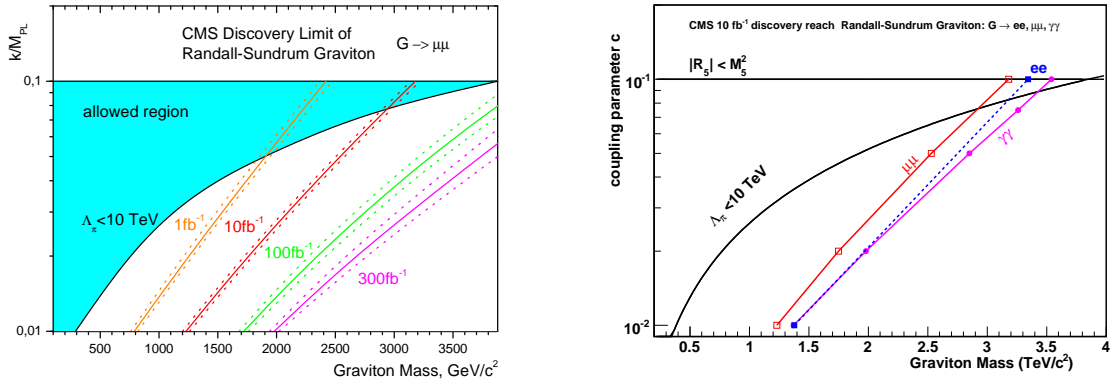


Figure 4: RS graviton discovery mass reach (at CMS) as a function of the model coupling parameter in the di-muon muon channel (left). The curves include the systematics uncertainty. On the right the comparison between the sensitivity of the different channels, shown for an integrated luminosity of 10 fb^{-1} .

At LHC the KK gravitons of RS1 would be seen as di-fermion or di-boson resonances. In particular, with early data, only the first excitation of the RS graviton can be accessible.

In Figure 4-(left) the reach of the CMS experiment⁵, for RS1 graviton in muon channel, is shown as a function of the coupling parameter (k/M_{PL} , where k is the curvature of the warped extra dimension and M_{PL} is the Planck mass in 5 dimensions) and the graviton mass. The ranges of the expected variations due to the systematic uncertainties are also drawn: 1 fb^{-1} is enough to explore a wide part of the region allowed by the theory.

Early data could not be enough to perform detailed angular distribution studies (crucial in order to distinguish a spin-1 particle, like the Z' , with respect to a spin-2 one, like the G_{RS}), however some handle is given by looking at resonances in some final states, which are precluded

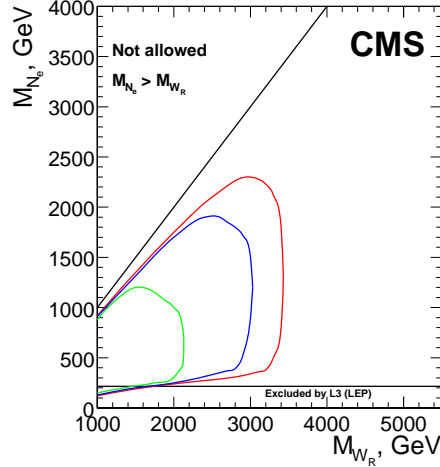


Figure 5: CMS discovery potential of the W_R boson and right-handed Majorana neutrinos of the Left-Right Symmetric model for an integrated luminosity of 1, 10 and 30 fb^{-1} .

in the other models due to the nature of the new particle. In fact, while the Z' cannot decay into a pair of vector bosons, the RS graviton can. In Figure 4-(right) the sensitivity of the analysis to the $G_{RS} \rightarrow \gamma\gamma$ channel is also drawn and shown to be comparable with the leptonic final states, thus allowing a cross-check of the resonance, even with a few collected data. The G_{RS} branching ratio to photons is roughly twice that of electrons or muons, however the reach for low coupling and graviton mass is comparable between di-leptons and di-photons due to the QCD and prompt photon backgrounds in the photon channel which are harder to efficiently suppress. For higher masses and coupling the di-photon is leading the reach due to the higher branching ratio. The di-muon channel is trailing the reach compared to the di-electrons merely due to resolution.

4 Two Leptons and Two Jets Final State

4.1 Heavy Majorana Neutrinos and right-handed bosons

The two leptons and two jets final states can be a clear signature of process described by left-right symmetric model $SU_c(3) \otimes SU_L(2) \otimes SU_R(2) \otimes U(1)$ ^{14,15}. The model embeds the SM at the scale of the order of 1 TeV and naturally explains the parity violation in weak interactions as a result of the spontaneously broken parity. It necessarily incorporates three additional gauge bosons W_R and Z' and the heavy right-handed Majorana neutrino states N . The N particles (N_l) can be the partners of the light neutrino states ν_l ($l = e, \mu, \tau$) and can provide their non-zero masses through the seesaw mechanism¹⁶.

The direct searches for W' at the Tevatron yield bounds $M_{W'} \gtrsim 720 \text{ GeV}/c^2$ assuming a light (keV-range) N , and $M_{W'} \gtrsim 650 \text{ GeV}/c^2$ assuming $M_N \gtrsim M_{W'}/2$ ¹⁷. These bounds are less stringent in more general LR models.

The cross section of $pp \rightarrow W_R \rightarrow l + N_l + X$, where $N_l \rightarrow l + j_1 + j_2$, depends on the value of the coupling constant g_R , the parameters of the CKM mixing matrix for the right-handed sector, the W_R - W_L and Z' - Z mixing strengths, and the masses of the partners N_l of the light neutrino state. In the study presented here the mixing angles are assumed small, the right-handed CKM matrix identical to the left-handed one and $g_R = g_L$. Finally it is assumed that only the lightest M_{N_e} is reachable at LHC. In the case of degenerated masses of N_l , the channels with μ 's and τ 's are open resulting in the increase of the cross section of the process studied here by a factor of 1.2. The two major backgrounds considered in this study are the inclusive production of Z

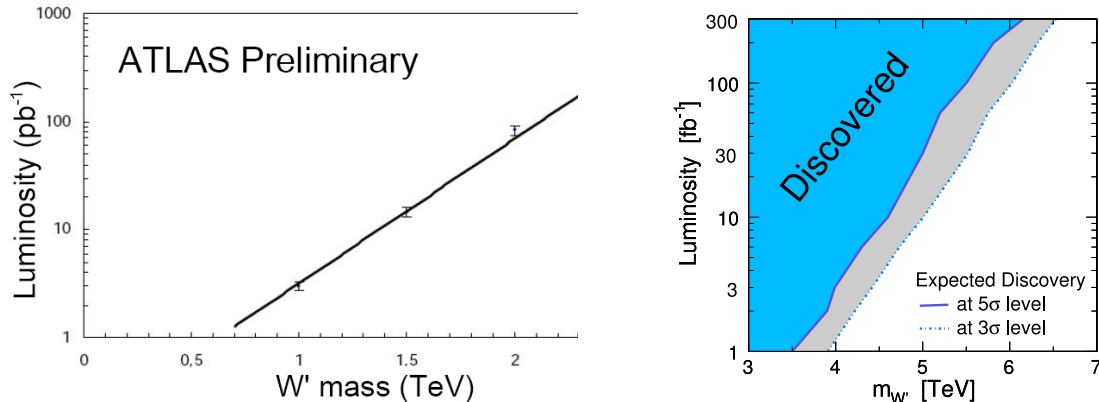


Figure 6: Integrated luminosity needed to discover (at 5 sigma level) a W' boson, depending on its mass, at ATLAS (left) and CMS (right).

and $t\bar{t}$. In the event selection two isolated electrons and at least two jets are required.

The 5 sigma discovery contour in the $(M_{W_R}; M_{N_e})$ plane is shown in Figure 5 for an integrated luminosity of 1, 10 and 30 fb^{-1} (CMS experiment simulation⁵). With 1 fb^{-1} a 5 sigma observation of W_R and N_e , with masses up to 2 TeV/c^2 and 1 TeV/c^2 respectively can be achieved.

5 Leptons and Missing Energy Final States

As mentioned in Section 3.1 many models predict additional heavy gauge boson, including charged particle. Here are presented the detection capabilities for a hypothetical heavy partner of the Standard Model W , a charged spin-1 boson W' , with the properties from the Reference Model by Altarelli¹⁸. In this model, the W' is a much massive copy of the W , with the very same left-handed fermionic couplings (including CKM matrix elements), while there is no interaction with the Standard Model gauge bosons or with other heavy gauge bosons as a Z' . Thus the W' decay modes and corresponding branching fractions are similar to those for the W . In hadron collisions W' bosons can be created through $q\bar{q}$ annihilation, in analogy to W production. Previous searches for the reference W' at LEP and at the Tevatron give rise to lower bounds approaching 1 TeV ¹².

Given that the W' boson has a large mass, it is likely to be produced without transverse momentum. Due to a boost along the z -axis, the angle between the muon and the neutrino might be different from π in the laboratory system. However, the angle in the transverse plane stays invariant under boosts along the z -axis. Therefore the signature of a W' event is high energy isolated muon, together with a large amount of missing energy pointing to the opposite direction in the transverse detector plane. Due to the small transverse momentum of the W' boson, the transverse momentum of the muon and the missing transverse energy are of similar magnitude.

In Figure 6 the discovery potential of both ATLAS¹⁹ and CMS⁵ is shown. Less than 1 fb^{-1} is needed to find a signal with a significance at 5-sigma level.

6 Black Hole

One of the consequence of large extra dimension is the possibility to produce microscopic black hole at LHC energy^{20,21}. From a semi-classical calculation the cross section of the black hole

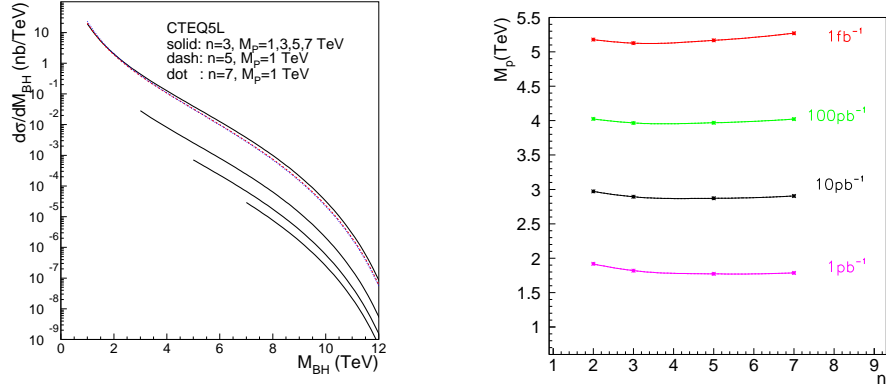


Figure 7: (Left) Differential cross section of the black hole production, as a function of a black hole mass for each (M_{PL}, n) parameter. (Right) Contours of the integrated luminosity needed for a 5 sigma discovery, plotted in the (M_{PL}, n) plane.

production can be written as

$$\sigma(M_{BH}) = \pi r_{s(4+n)}^2$$

where $r_{s(4+n)}^2$ is the Schwarzschild radius in “4+n” dimensions.

Considering a black hole mass much larger than the Planck mass in 4+n dimensions (M_{PL}), and assuming the latter to be of the order of the TeV scale, then $\sigma(M_{BH}) \sim \text{pb}^a$.

The black holes have a very short life time, predicted to be of the order of 10^{-12} fs and are expected to evaporate democratically by emission of all particle types that exist in nature, independent of their quantum numbers or interaction properties. Therefore they can be a source of new particles. Black holes would also be able to provide the possibility of probing quantum gravity.

Requiring M_{BH} to be larger than M_{PL} , potentially the black hole observation can be accomplished within an integrated luminosity of 1 fb^{-1} in all cases of n and if M_{PL} is less than 5 TeV, as shown in Figures 7.

7 Summary

The Large Hadron Collider will give the possibility to shade light on new physics and models. Here some examples of the phenomena that could be discovered with few data collected at ATLAS and CMS have been reviewed. In Table 1 a summary of such discoveries are reported. Although the understanding of the detector will be crucial for a claim of an observation of a new signal, both experiment show a high discovery potential already with an integrated luminosity of few fb^{-1} .

^aRecent studies claims that due to the “Apparent Horizon” effect, the event horizon is not formed as fast as needed, thus a large fraction of the initial energy could escape before the black hole is formed. This implies that more partonic energy is needed to form the black hole than the one predicted by the naive semi-classical calculation. In such a scenario the black hole cross section is a few orders of magnitude smaller than the above calculation.

Table 1: Summary of the principal discoveries accessible with the first data taken at LHC.

Model	Mass Reach (TeV)	L (pb ⁻¹)	Early Systematic
Contact interaction	$\Lambda \sim 2.8$	10	Jet efficiency and energy scale
Z'			
ALRM	M \sim 1	10	Alignment
SSM	M \sim 1	20	
LRM	M \sim 1	30	
E ₆ , SO(10)	M \sim 1	30-100	
Technirho	M \sim [0.3]	100	Jet energy scale
Axigluon or Colouron	M \sim [0.7,3.5]	100	Jet energy scale
Excited quark	M \sim [0.7,3.6]	100	Jet energy scale
E ₆ di-quarks	M \sim [0.7,4]	100	Jet energy scale
mUED	M \sim 0.3 – 0.6	10-1000	MET, jet/photon energy scale
ADD real G_{KK}	M _D \sim 1.5 (n=3), \sim 1 (n=6)	100	MET, jet/photon energy scale
ADD virtual G_{KK}	M _D \sim 4.3 (n=3), \sim 3 (n=6)	100	Alignment
	M _D \sim 5 (n=3), \sim 4 (n=6)	1000	
RS1			
di-jets	M _G \sim [0.7,0.8], c=0.1	100	Jet energy scale, alignment
di-muons	M \sim [0.8,2.3], c=[0.01,0.1]	1000	

References

1. S. Tsuno, this proceedings.
2. The CMS Collaboration, CMS PAS SBM 07 001 (2007).
3. N. Krasnikov and V. Matveev, *Phys. Usp.* **47**, 643 (2004).
4. K. Gumus *et al.*, CMS Note 2006/070 (2006), and references therein.
5. The CMS Collaboration, CERN/LHCC 2006-021, CMS TDR 8.2 (2006).
6. B. Clerbaux *et al.*, CMS Note 2006/004 (2006).
7. M. Cvetič and P. Langacker *Phys. Rev. D* **54**, 3570 (1996).
8. M. Cvetič and P. Langacker *Mod. Phys. Lett. A* **11**, 1247 (1996).
9. A. Leike *Phys. Rept.* **317**, 143 (1999).
10. C.T. Hill and E.H. Simmons, *Phys. Rept.* **381**, 235 (2003).
11. T. Han *et al.*, *Phys. Rev. D* **67**, 095004 (2003).
12. W.M. Yao *et al.*, *JPG* **33**, 1 (2006) and 2007 partial update for 2008.
13. L. Randall, this proceedings.
14. R. Mohapatra and J. Pati, *Phys. Rev. D* **11**, 566 (1975).
15. G. Senjanovic and R. Mohapatra, *Phys. Rev. D* **12**, 1502 (1975).
16. R. Mohapatra and G. Senjanovic, *Phys. Rev. Lett.* **44**, 912 (1980).
17. D0 Collaboration, S. Abachi *et al.*, *Phys. Rev. Lett.* **76**, 3271 (1996).
18. G. Altarelli *et al.*, *ZPC* **45**, 109 (1989).
19. The ATLAS Collaboration, CERN/LHCC 99-015, ATLAS TDR 15 (1999).
20. S. Dimopoulos and G. Landsberg, *Phys. Rev. Lett.* **87**, 161602 (2001).
21. B. Giddings and S. Thomas, *Phys. Rev. D* **65**, 056010 (2002).